Journal of Orthopaedic Science xxx (xxxx) xxx

Contents lists available at ScienceDirect

Journal of Orthopaedic Science

journal homepage: http://www.elsevier.com/locate/jos

Original Article

Three-dimensional morphological analysis of cervical foraminal stenosis using dynamic flexion-extension computed tomography images

Tatsuki Mizouchi [a, *], Keiichi Katsumi [b], Tomohiro Izumi [c], Akiyoshi Yamazaki [b], Hirokazu Shoji [d], Hideki Tashi [a], Masayuki Ohashi [a], Toru Hirano [e], Naoto Endo [a], Kei Watanabe [a]

[a] Department of Orthopedic Surgery, Niigata University, Medical and Dental General Hospital, 1-757 Asahimachidori, Chuoku, Niigata City, Niigata, 951-8510, Japan
[b] Spine Center, Department of Orthopedic Surgery, Niigata Central Hospital, 1-18 Shinko-cho, Chuoku, Niigata City, Niigata, 950-8556, Japan
[c] Department of Orthopedic Surgery, Niigata Minami Hospital, 2007-6 Toyano, Chuoku, Niigata City, Niigata, 950-8601, Japan
[d] Department of Orthopedic Surgery, Niigata City General Hospital, 463-7 Shumoku, Chuoku, Niigata City, Niigata, 950-1197, Japan
[e] Department of Orthopedic Surgery, Uonuma Institute of Community Medicine, Niigata University Medical and Dental Hospital, 4132 Urasa, Minami-uonuma City, Niigata, 949-7302, Japan

ARTICLE INFO

Article history:
Received 28 July 2019
Received in revised form
18 September 2019
Accepted 5 November 2019
Available online xxx

ABSTRACT

Background: Morphological features of foraminal stenosis in cervical spondylotic radiculopathy and the adequate extent of facet resection in posterior cervical foraminotomy remain uncertain. Herein, we evaluated quantitatively foraminal widths in cervical spondylotic radiculopathy on dynamic flexion-extension computed tomography using a novel three-dimensional analysis method and determined the extent of facet resection in posterior cervical foraminotomy.

Methods: Seventeen patients undergoing posterior cervical foraminotomy for cervical spondylotic radiculopathy were evaluated. A neuroforamen three-dimensional model was built from preoperative images of flexion-extension computed tomography myelography, and an ordinary cervical spine coordinate system and an original neuroforaminal coordinate system, were established. In the neuroforaminal coordinate system, minimum areas perpendicular to the long axis by the slices from inlet to outlet of neuroforamen and narrowest foraminal width in a slice of minimum area were measured. The location of the narrowest region from inlet of the foramen was calculated. Ratios of minimum and sufficient facet resection were obtained from the location of the narrowest region in the neuroforaminal coordinate system.

Results: The narrowest foraminal widths (flexion/extension) in the cervical spine coordinate system and the neuroforaminal coordinate system were 2.9/2.3 and 2.6/1.9 mm, respectively. The mean values of the location of the narrowest region (flexion/extension) were 0.27/0.22 and 0.50/0.45 mm, respectively, and the narrowest region in the neuroforaminal coordinate system was located on the outer side than in the cervical spine coordinate system ($p < 0.001$). The ratios of minimum and sufficient facet resection were 23 ± 8% and 32 ± 9%, respectively.

Conclusions: The narrowest regions both in flexion and extension are located at the middle of the foramen based on the neuroforaminal coordinate system. Ordinary evaluation of axial computed tomography images likely underestimates the extent of facet resection, whereas certain extent of facet resection does not exceed 50% in cases with single-level cervical spondylotic radiculopathy.

Study design: A retrospective case control study.

* Corresponding author. Department of Orthopedic Surgery, Niigata University, Medical and Dental General Hospital, 1-757 Asahimachidori, Chuoku, Niigata City, Niigata, 951-8510, Japan. Fax: +81 25 227 0782.
E-mail address: mizochi07@gmail.com (T. Mizouchi).

https://doi.org/10.1016/j.jos.2019.11.002
0949-2658/

1. Introduction

Cervical spondylotic radiculopathy (CSR) is characterized by narrowing of the intervertebral foramen owing to degenerative changes. The symptoms usually improve in the flexed position and worsen in the extended position [1]. For resistant radicular pain or muscle weakness, surgical treatment is occasionally indicated. Anterior cervical discectomy with fusion has been established as an effective procedure for CSR, despite the fact that it requires sacrifice of the mobile segment or specific techniques to directly decompress the nerve root through an anterior approach. Posterior cervical foraminotomy has been established as an alternative, less-invasive procedure that permits preservation of the mobile segment and securely decompresses the entrapped nerve root [2,3]. With regard to adequate extent of foraminal decompression, posterior cervical foraminotomy should be limited to resecting less than half of the intervertebral facet joint to prevent segmental instability according to previous biomechanical studies [4]. However, posterior central canal decompression with single unilateral total facetectomy and single- or multilevel posterior cervical foraminotomy does not adversely affect clinical outcomes or segmental stability in the clinical setting [2,5–7]. Therefore, a new principle to determine the adequate extent of foraminal decompression is needed.

Currently there is a lack of high-precision imaging techniques needed to make the necessary anatomical evaluations. For instance, assessments in previous studies have been based on two-dimensional image analyses of foraminal stenosis using plain computed tomography (CT) that cannot make accurate evaluations of anatomical structures [8–10]. Therefore, we introduced a novel CT based three-dimensional (3D) analysis method to visualize the neuroforamen and enable accurate measurement of stenotic regions. Our first aim was to use our 3D analysis method to evaluate dynamic flexion-extension CT images, and to precisely measure the neuroforaminal stenotic parameters in patients with CSR. Second, we aimed to evaluate the adequate extent of facet resection based on the aforementioned anatomical evaluation.

2. Materials and methods

2.1. Study population

This study was approved by the institutional review board of our institution, and informed consent was obtained from all participants. As a symptomatic group, seventeen patients (15 males, two females; average age at surgery: 51.5 ± 10.0 years; average body mass index: 24.1 ± 4.2 kg/m^2) were recruited from a single spine center between January 2008 and December 2016. They all suffered from radiculopathy with positive Spurling tests or Jackson compression tests because of degenerative neuroforaminal stenosis at single C5-6 or C6-7 level. Dynamic flexion and extension computed tomography myelography (CTM) was obtained before surgery, and 17 symptomatic foramina were evaluated. All patients underwent single-level posterior cervical foraminotomy which relieved them of their radicular pain.

As a control group, five patients (all males, average age at surgery: 51.8 ± 6.2 years, average body mass index: 27.5 ± 3.9 kg/m^2) with cervical disk intraforaminal herniation at other than C5-6 or C6-7 levels were recruited during the same period. They showed less degenerative change of intervertebral discs at C5-6 and C6-7 levels with Pfirrmann classification from grade I to III on magnetic resonance imaging [11]. They underwent dynamic flexion-extension CTM preoperatively, and 10 target foramina at C5-6 and C6-7 levels on the asymptomatic side were evaluated. Demographic data of the symptomatic and control groups are shown in Table 1.

Table 1
Demographic data in the two groups.

	Symptomatic group (n = 17)	Control group (n = 5)
Number of foramina	17	10
Level	C5-6: 7, C6-7: 10	C5-6: 5, C6-7: 5
Evaluated side (Right)	7	6
Sex (male)	15	all
Age at surgery (years), mean ± SD	51.5 ± 10.0	51.8 ± 6.2
Body mass index (kg/m^2), mean ± SD	24.1 ± 4.2	27.5 ± 3.9
Visual analog scale, mean ± SD		
Pain/stiffness in neck/shoulder pre-op	56 ± 21 mm*	–
Pain/stiffness 6 months post-op	22 ± 28 mm*	–
Pain/numbness in arms/hands pre-op	58 ± 17 mm†	–
Pin/numbness 6 months post-op	15 ± 25 mm†	–

Abbreviations: pre-op, preoperatively; post-op, post-operatively; SD, standard deviation.
*p = 0.002, †p < 0.001.

2.2. CT evaluation of neuroforamen

CTM examination was performed using a 16-row CT system (Aquilion; Toshiba Medical System Corporation, Tochigi, Japan). The imaging conditions with the system were as follows: mean pixel size, 0.29 mm^2 (range: 0.23–0.35); slice thickness, 0.5 mm; slice increment, 0.5 mm; voltage, 120 kV; current, 300 mA. The extended position was acquired as patients stuck their chin out in the prone position, while the flexed position was obtained as they put their chin down with a pillow as much as possible.

From acquired CT DICOM data of the cervical spine in each full flexion and full extension position, a 3D cervical spine model was created automatically (the default bone threshold: 226–1736 HU) using MIMICS® software (Materialise Japan Co., Ltd., Yokohama, Japan). The lower vertebral body of the model in extension was superimposed semi-automatically on the model in flexion, and intra-foraminal area was calculated in both flexion and extension. The lower vertebral body indicated C6 in cases of C5-6 CSR, and C7 in cases of C6-7 CSR.

We defined two rectangular coordinate systems to evaluate 3D structures of the neuroforamen. One was the cervical spine coordinate system (CCS), defined as follows: a plane bisected the lower vertebral body (Fig. 1-A; green line), and another plane passed through the intervertebral disc including the target neuroforamen (Fig. 1-A; red line). This coordinate system aimed to evaluate foraminal stenosis on the axial views as in ordinary clinical use. The other was the neuroforamen coordinate system (NCS) to evaluate the 3D structures of neuroforamen more precisely, defined as follows: a first plane based on the central line of the lower pedicle, a second plane aligned parallel to the first plane touching the inner borders of the ipsilateral upper and lower pedicles (Fig. 1-B; blue line), and a third plane fixed perpendicular to each ipsilateral upper and lower pedicle (Fig. 1-B; yellow line). This coordinate system aimed to evaluate foraminal stenosis accurately along the long axis of the neuroforamen. The border of the neuroforamen consisted of the following components: 1) Top: inferior edge of the upper pedicle; 2) Anterior wall: uncovertebral joint; 3) Bottom: the superior edge of the lower pedicle; 4) Posterior wall: the anterior margin of the pars interarticularis; and 5) the superior articular process.

2.3. Measurement of the neuroforamen in the cervical spine coordinate system

In the CCS, foraminal width and location of the narrowest region within the neuroforamen were calculated on axial images. The foraminal width was calculated automatically in all distances

Please cite this article as: Mizouchi T et al., Three-dimensional morphological analysis of cervical foraminal stenosis using dynamic flexion-extension computed tomography images, Journal of Orthopaedic Science, https://doi.org/10.1016/j.jos.2019.11.002

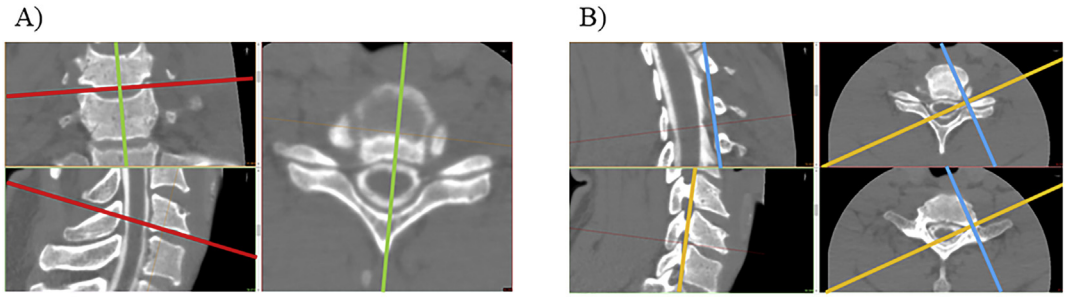

Fig. 1. A) Cervical spine coordinate system: Green plane aligned along the center of the vertebral body. Red plane aligned along the intervertebral disc. B) Neuroforamen coordinate system: Blue plane aligned along the central line of the lower pedicle and parallel to the plane touching the inner edges of upper and lower pedicles. Yellow plane was fixed perpendicular to each upper and lower pedicle. (For interpretation of the references to color in this figure legend, the reader is referred to the Web version of this article.)

between anterior contour pixels and posterior distances of binary contour neuroforamen images using an original program written in MATLAB (MathWorks Inc., MA, USA). The location of the narrowest region was obtained from the following formula: distance from inlet to the narrowest region/total distance along the long axis of neuroforamen. This means that the slice of interest was located close to the inlet of the neuroforamen if the value was close to 0, and close to the outlet if the value was close to 1. These measurements and calculations were performed in flexion and extension separately.

2.4. Measurement of the neuroforamen in neuroforamen coordinate system

In the NCS, the neuroforamen 3D model was created by subtracting the cervical spine 3D model from the cervical spine 3D model that contained the neuroforaminal space (Fig. 2). Intraforaminal areas in each slice per pixel along the long axis from inlet to outlet were calculated by the software. Minimum area, inlet and outlet area were evaluated, and location of the narrowest region within the neuroforamen was calculated. The location of the narrowest region was obtained from the following formula: distance from the inlet to the minimum area slice/total distance along the long axis of the neuroforamen. This means that the interest slice was located close to the inlet of the neuroforamen if the value was close to 0, and close to the outlet if the value was close to 1 (Fig. 3).

Similar to the CCS, five parameters of foraminal width along the antero–posterior axis were calculated using MATLAB from binarized images at the following five levels: D1, superior articular process; D2, uncinate joint; D3, midpoint between the top and the uncinate joint; D4, midpoint between the uncinate joint and the bottom; and D5, the centroid of the foramen. The foraminal width in the narrowest region was detected using these five parameters (Fig. 4). These measurements and calculations were performed in flexion and extension, separately. Finally, the coincidence rates among the five parameters (from D1 to D5) between the narrowest parameters in flexion and those in extension, and the distribution of stenotic levels were calculated.

2.5. Adequate extent of facet resection in the cervical spine coordinate system

In the NCS, the neuroforamen 3D model in the extension position was divided into three parts: medial (green), middle (pink), and lateral (blue) parts. The medial part indicates the space between the inlet and narrowest region in extension, and the lateral part indicates the space between the outlet and the safety region with same area as narrowest region in flexion (Fig. 5-A). Because radiculopathy reduced in the flexed position, the minimum area in flexion position was considered to be the threshold value of the intra-foraminal area indicating sufficient decompression of the nerve root. Finally, the 3D model was converted to the CCS (Fig. 5-

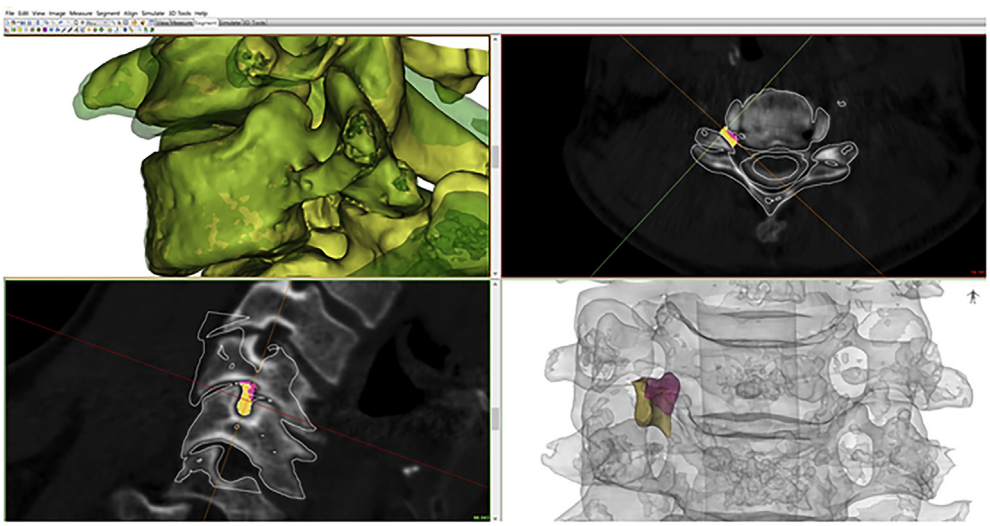

Fig. 2. 3D neuroforamen model was created using MIMICS® software, and lower vertebral body of the model in extension was superimposed on the model in flexion, and intraforaminal area was calculated. The orange part indicates extension. Pink plus orange indicates flexion.

Please cite this article as: Mizouchi T et al., Three-dimensional morphological analysis of cervical foraminal stenosis using dynamic flexion-extension computed tomography images, Journal of Orthopaedic Science, https://doi.org/10.1016/j.jos.2019.11.002

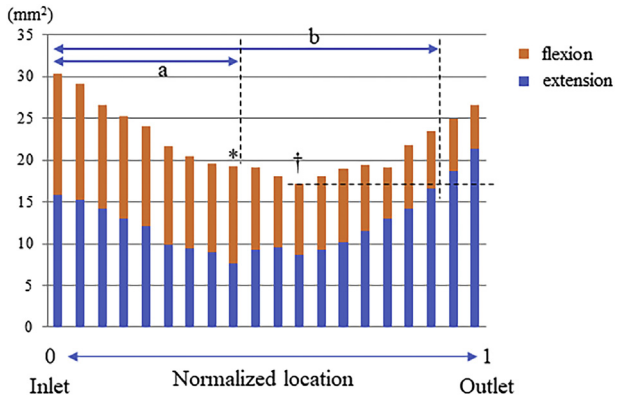

Fig. 3. Intra-foraminal areas per slices. **a** and **b** indicate the distances from inlet to the narrowest region in extension (*) and from inlet to the region in the extension with same area as the minimum area in the flexion (†).

B), and a length from the inner edge of the facet joint to the narrowest region (Fig. 5-B(a)), a length from inner edge of facet joint to the safety region (Fig. 5-B (b)), and a total length from inner to the outer edge of the facet joint (Fig. 5-B (c)) along the horizontal axis were calculated. Ratios of minimum and sufficient facet resection were calculated to confirm adequate extent of facet resection on ordinary axial CT images using the formula: a/c × 100 (%), and b/c × 100 (%).

2.6. Actual facet resection after foraminotomy

To assess the actual facet resection after surgery, a length of the resected facet joint was measured on axial CT images in the CCS, and the ratio of actual facet resection was calculated using the following formula: [1 − (length of resected facet joint)/(total length from inner to the outer edge of the facet joint before surgery)] × 100 (%).

2.7. Surgical procedure

The foraminotomy containing C5-6 or C6-7 foramen was performed under microscopy using a high-speed drill with a 2-mm diamond burr and a microsharp curette. The medial facet joints, including both superior and inferior articular processes, were resected to the extent that a microball tip (1 mm) could be inserted easily around the nerve root.

2.8. Statistical analysis

The differences between the symptomatic and control groups and the changes in investigated parameters of CT from flexion to extension were evaluated using the parametric two sample t-test and paired t-test respectively. Data were analyzed using the SPSS 22 statistical software package (SPSS, Inc., Chicago, IL), and p values < 0.05 were considered to indicate statistical significance.

3. Results

Radiological parameters in both CCS and NCS are shown in Table 2. There were no significant differences of foraminal widths in the CCS between the symptomatic and the control groups. In NCS, minimum area, foraminal width of D2 and the narrowest width within the minimum area from D1 to D5 in the symptomatic group were significantly smaller than those in the control group (all comparisons, ps < 0.05).

3.1. Foraminal width

In the CCS, foraminal widths were found to be significantly smaller in extension (flexion: 2.9 mm, extension: 2.3 mm; $p = 0.014$). In the NCS, foraminal widths at all five levels were significantly smaller in extension (flexion (D1-D5): 5.2, 3.0, 5.3, 3.7, 3.8 mm; extension (D1-D5): 4.0, 2.4, 3.4, 3.3, 3.4; ps < 0.05). The narrowest width from D1 to D5 was also significantly smaller in extension (flexion: 2.6 mm, extension: 1.9 mm, $p = 0.001$). However, there was no significant difference between the foraminal width in extension in the CCS and the narrowest width in the NCS ($p = 0.77$). Coincidence rate between the narrowest parameter from D1 to D5 in flexion and that in extension was 53%. The distribution of stenotic levels, including duplication of the narrowest width in flexion, was D1 6%, D2 53%, D3 0%, D4 47%, and D5 12%, and that in extension was D1 12%, D2 53%, D3 18%, D4 29%, and D5 0%.

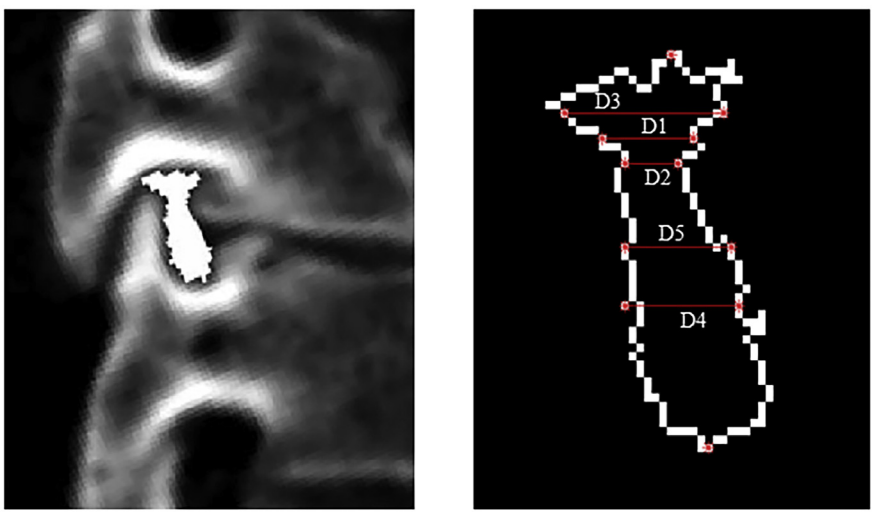

Fig. 4. Measurement of the foraminal width in a slice of minimum area at five levels (from D1 to D5) using an original program written in MATLAB.

Please cite this article as: Mizouchi T et al., Three-dimensional morphological analysis of cervical foraminal stenosis using dynamic flexion-extension computed tomography images, Journal of Orthopaedic Science, https://doi.org/10.1016/j.jos.2019.11.002

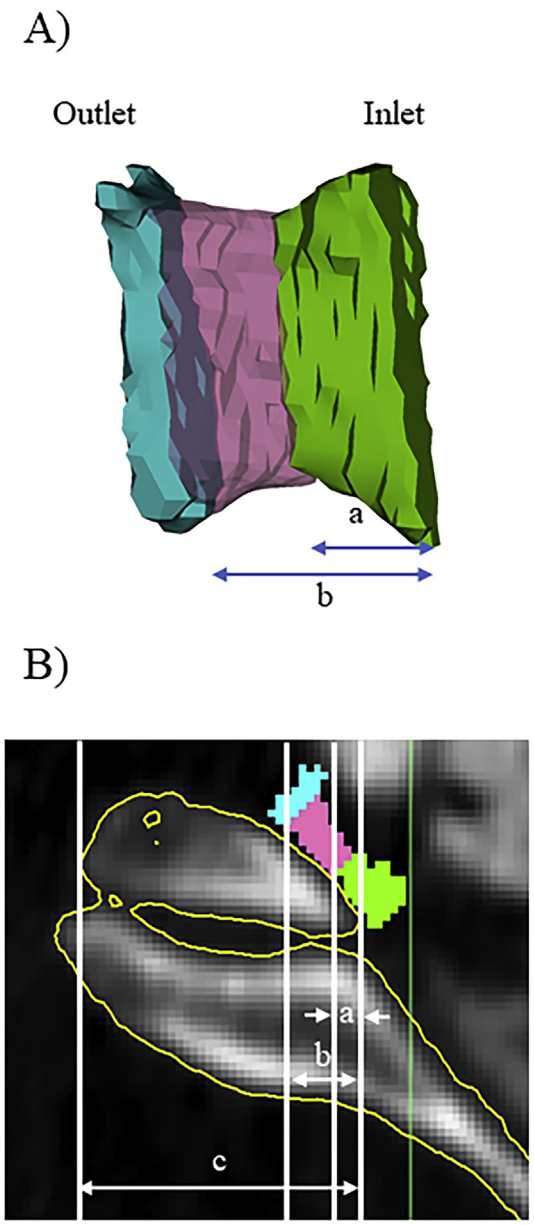

Fig. 5. A) The 3D extension foramen model was divided into medial (green), middle (pink), and lateral (blue) parts according to **a** and **b** that indicate spaces between the inlet and narrowest region and between the inlet and safety region, respectively. B) When the 3D model was converted to the ordinal axial image, **a**, **b**, and **c** indicate lengths from the inner edge of the facet joint to the narrowest region, to the safety region, and the total facet joint, respectively.

3.2. Location of the narrowest region

In the CCS, the location of the narrowest region (flexion/extension) was 0.27/0.22 on average ($p = 0.16$). In the NCS, the location of the narrowest region (flexion/extension) was 0.50/0.45 on average ($p = 0.03$), suggesting that the narrowest region in the NCS was located closer to the outlet than in the CCS ($p < 0.001$) (Fig. 6).

3.3. Adequate extent of facet resection in cervical spine coordinate system

The lengths from the inner edge of the facet joint to the narrowest and safety regions were 6.3 ± 0.6 mm and 7.5 ± 1.9 mm, respectively. The ratios of minimum and sufficient facet resection were 23 ± 8% (range, 5%–42%), and 32 ± 9% (range, 15%–49%), respectively (Table 3).

Table 2
Radiographic evaluation of cervical foraminal stenosis.

		Symptomatic group (mean ± SD)	Control group (mean ± SD)	p value
Cervical spine coordinate system				
Foraminal width (mm)				
flexion		2.9 ± 1.2	3.4 ± 1.6	0.32
extension		2.3 ± 1.0[a]	3.1 ± 1.7[a]	0.11
Location of narrowest region				
flexion		0.27 ± 0.15	0.40 ± 0.18	0.069
extension		0.22 ± 0.16	0.38 ± 0.20[a]	0.028*
Neuroforaminal coordinate system				
Foraminal width (mm)				
D1	flexion	5.2 ± 1.9	6.2 ± 2.7	0.24
	extension	4.0 ± 2.3[a]	4.3 ± 2.2[a]	0.71
D2	flexion	3.0 ± 1.4	4.5 ± 1.4	0.015*
	extension	2.4 ± 1.4[a]	3.9 ± 1.7	0.019*
D3	flexion	5.3 ± 1.9	6.3 ± 2.2	0.22
	extension	3.4 ± 1.9[a]	4.6 ± 2.3[a]	0.16
D4	flexion	3.7 ± 1.0	4.1 ± 0.9	0.31
	extension	3.3 ± 0.8[a]	3.8 ± 1.2	0.21
D5	flexion	3.8 ± 1.2	5.5 ± 1.8	0.008**
	extension	3.4 ± 1.3	4.4 ± 1.6[a]	0.078
Narrowest width in D1-5				
flexion		2.6 ± 1.0	3.8 ± 1.1	0.006**
extension		1.9 ± 1.1[a]	3.1 ± 1.3[a]	0.022*
Intra-foraminal area along long axis (mm^2)				
Minimum area				
flexion		21.6 ± 4.7	27.2 ± 6.9	0.02*
extension		16.2 ± 4.5[a]	20.2 ± 6.5[a]	0.076
Inlet area				
flexion		41.6 ± 8.9	49.7 ± 14.5	0.08
extension		31.1 ± 10.7[a]	37.0 ± 15.9[a]	0.26
Outlet area				
flexion		44.0 ± 12.2	52.2 ± 8.3	0.072
extension		39.0 ± 10.5[a]	48.9 ± 8.3[a]	0.018*
Location of narrowest region				
flexion		0.50 ± 0.05	0.49 ± 0.11	0.76
extension		0.45 ± 0.08[a]	0.39 ± 0.11[a]	0.15
Total distance along long axis (mm)		6.0 ± 0.9	5.8 ± 1.0	0.54

Abbreviations: SD, standard deviation.
*$p < 0.05$, **$p < 0.01$.
[a] The radiographic parameter in extension was significantly less than that in flexion ($p < 0.05$).

3.4. Actual facet resection after foraminotomy in cervical spine coordinate system

The ratio of actual facet resection was 47 ± 11% (range, 29%–68%). The ratios of actual facet resection in all patients were higher than the ratios of sufficient facet resection expected from preoperative CT images (Table 3).

4. Discussion

4.1. Evaluation of neuroforaminal stenotic regions using the novel 3D analysis method

In this study, a 3D model was established from flexion-extension CT images in which the narrowest region within the foramen could be visualized in the NCS. The narrowest foraminal widths in extension were significantly shorter than those in flexion, which was compatible with findings of clinical practice where deteriorating radiculopathy causes the foraminal width to be narrower in the extended position [1]. In 3D analysis of the narrowest foraminal width, stenotic level was most frequently located at the uncinate

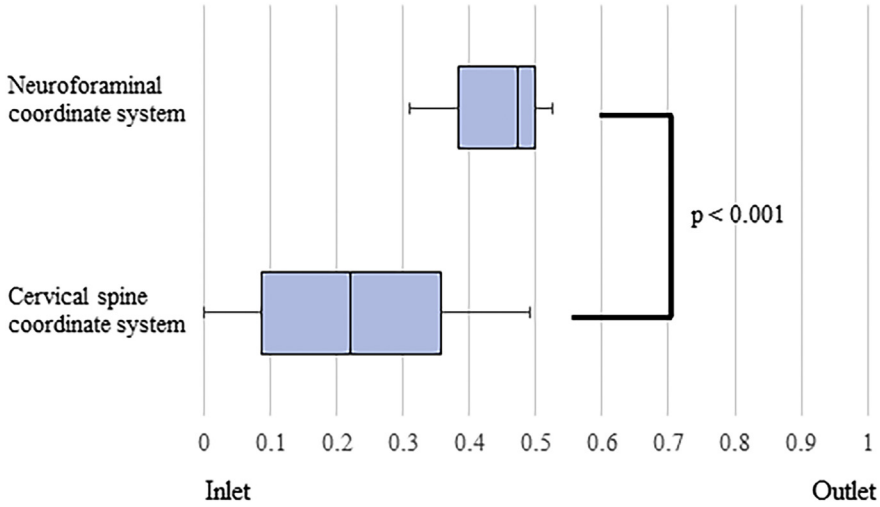

Fig. 6. Comparison of the location of the narrowest region in extension between the cervical spine and neuroforaminal coordinate system. The narrowest region in the neuroforaminal coordinate system was located on the outer side than in the cervical spine coordinate system.

joint, whereas the distribution of the stenotic levels was unequal between the top and the bottom of the neuroforamen.

As for cervical foraminal stenosis, several reports emphasized that evaluation of multi-planar views or 3D images was better than that of single axial or sagittal views [9,12,13]. Although the benefits of oblique reformation perpendicular to the long axis of the neural foramen were reported for both diagnosis and evaluation of stenotic lesions using CT and MRI [8,10], MRI analysis is limited in terms of evaluating bone structures in detail [3,9,14]. In addition, few studies have been conducted to quantitatively evaluate the anatomy and severity of stenotic regions using CT image analysis in cervical foraminal stenosis. Therefore, we conducted quantitative evaluations using our 3D analysis method that resolves previous problems by measuring dynamic changes in the intra-foraminal area. In this study, CTM was used because it was taken routinely to assess cervical cord entrapment; however, plane CT can be substituted for CTM in our 3D analysis method.

A previous cadaveric study demonstrated that the diameters of C6 and C7 nerve roots were 5.8 mm and 4.8 mm, respectively [15]. Foraminal widths in this study were small enough to suffer from nerve root entrapment. This study also demonstrated changes of intra-foraminal area and width from flexion to extension. Although the location of the narrowest region did not change regardless of cervical position, the distributions of the stenotic levels from D1 to D5 were unequal between flexion and extension. Since the anatomical structures compressing the nerve root in the foramina vary among individuals, these measurements can be used to recommend the extent of resection from upper and lower pedicles needed to achieve a certain level of decompression in the vertical direction [16].

4.2. Adequate extent of facet resection in the inside and outside directions

Significantly, we found that the narrowest region was located on the outer side in the NCS, compared to its more inner location in the CCS. This mismatch in location, clarified using our 3D image analysis, might lead to insufficient decompression in posterior cervical foraminotomy. When the location of the narrowest region was converted from the NCS into CCS, the ratio of sufficient facet resection ranged from 15% to 49%.

Previous studies suggested that the ratio of facet resection should be approximately one-third to half to avoid postoperative intervertebral instability [4] and to achieve good clinical outcomes [2,16–18]. In this study, the ratio of actual facet resection was 47 ± 11% (range, 29%–68%), which was sufficient based on current knowledge. However, due to a lack of high-precision imaging tools, only a few studies have performed anatomical evaluation before surgery and reported morphologic characteristics such as simple classification of cervical foraminal stenosis. Gu et al. [19] morphologically classified two types (v-shaped and parallel-shaped foraminal stenoses) on ordinal CT axial images and reported a higher possibility of insufficient decompression in parallel-shaped foraminal stenosis. The present study first showed that the ratio of sufficient facet resection was 32% on average, ranging from 15% to 49%, from the anatomical viewpoint of quantitative evaluation. These facts are important for preoperative evaluation, and an extent of resection up to 50% can be recommended to achieve sufficient decompression in cases with single-level cervical foraminal stenosis. This guideline is consistent with our practical experience of actual facet resection in the present study. However, in cases with severe degenerative changes with multiple discs or facet lesions, more than half of the facet joint may need to be resected.

Table 3
Ratios of facet resection.

	Ratio (mean ± SD)	Range
Minimum facet resection (%)	23 ± 8	5–42
Sufficient facet resection (%)	32 ± 9	15–49
Actual facet resection (%)	47 ± 11	29–68

Abbreviations: SD, standard deviation.

4.3. Limitations

The present study has several limitations. First, the sample size was too small to analyze other contributing factors such as age, sex, body mass index, and severity of facet degeneration in the symptomatic group. Although these matters need further investigation using larger sample sizes or including various degenerative changes in the future, this study provided informative morphologic features of cervical foraminal stenosis based on a relatively homogeneous patient population, without central canal stenosis or intra-foraminal disc herniation. Second, because the evaluation was performed using only CT images, soft tissues such as ligaments and bulging discs could not be evaluated, both of which potentially contribute to nerve root compression. Therefore, further study, in

Please cite this article as: Mizouchi T et al., Three-dimensional morphological analysis of cervical foraminal stenosis using dynamic flexion-extension computed tomography images, Journal of Orthopaedic Science, https://doi.org/10.1016/j.jos.2019.11.002

combination with high-resolution MRI or image matching methods, is needed to improve the precision of the evaluations.

In summary, our 3D model could visualize and quantitatively evaluate the narrowest region within the neuroforamen in both flexion and extension. The narrowvest foraminal widths in extension were significantly less than those in flexion. In the NCS, the narrowest regions in both flexion and extension were located at the middle of the neuroforamen on average. The ordinary evaluation on axial CT images was very likely to underestimate the extent of facet resection, whereas sufficient extent of facet resection did not exceed 50% in this series.

Ethical approval

All procedures performed in studies involving human participants were in accordance with the ethical standards of the institutional and/or national research committee and with the 1964 Helsinki declaration and its later amendments or comparable ethical standards.

Funding

None.

Financial/Conflict of interest

None reported.

References

[1] Rhee JM, Yoon T, Riew KD. Cervical radiculopathy. J Am Acad Orthop Surg 2007 Aug;15(8):486–94.
[2] Baba H, Chen Q, Uchida K, Imura S, Morikawa S, Tomita K. Laminoplasty with foraminotomy for coexisting cervical myelopathy and unilateral radiculopathy: a preliminary report. Spine (Phila Pa 1976) 1996 Jan 15;21(2):196–202.
[3] Bartlett RJ, Hill CA, Devlin R, Gardiner ED. Two-dimensional MRI at 1.5 and 0.5 T versus CT myelography in the diagnosis of cervical radiculopathy. Neuroradiology 1996 Feb;38(2):142–7.
[4] Zdeblick TA, Zou D, Warden KE, McCabe R, Kunz D, Vanderby R. Cervical stability after foraminotomy. A biomechanical in vitro analysis. J Bone Joint Surg Am 1992 Jan;74(1):22–7.
[5] Lee DH, Cho JH, Hwang CJ, Lee CS, Kim C, Ha JK. Multilevel posterior foraminotomy with laminoplasty versus laminoplasty alone for cervical spondylotic myelopathy with radiculopathy: a comparative study. Spine J 2018 Mar;18(3):414–21.
[6] Nakamura M, Iwanami A, Tsuji O, Hosogane N, Watanabe K, Tsuji T, Ishii K, Toyama Y, Chiba K, Matsumoto M. Long-term surgical outcomes of cervical dumbbell neurinomas. J Orthop Sci 2013 Jan;18(1):8–13.
[7] Ohashi M, Yamazaki A, Watanabe K, Katsumi K, Shoji H. Two-year clinical and radiological outcomes of open-door cervical laminoplasty with prophylactic bilateral C4-C5 foraminotomy in a prospective study. Spine (Phila Pa 1976) 2014 Apr 20;39(9):721–7.
[8] Flannigan BD, Lufkin RB, McGlade C, Winter J, Batzdorf U, Wilson G, Rauschning W, Bradley Jr WG. MR imaging of the cervical spine: neurovascular anatomy. AJR Am J Roentgenol 1987 Apr;148(4):785–90.
[9] Kaiser JA, Holland BA. Imaging of the cervical spine. Spine (Phila Pa 1976) 1998 Dec 15;23(24):2701–12.
[10] Roberts CC, McDaniel NT, Krupinski EA, Erly WK. Oblique reformation in cervical spine computed tomography: a new look at an old friend. Spine (Phila Pa 1976) 2003 Jan 15;28(2):167–70.
[11] Pfirrmann CW, Metzdorf A, Zanetti M, Hodler J, Boos N. Magnetic resonance classification of lumbar intervertebral disc degeneration. Spine (Phila Pa 1976) 2001 Sep 1;26(17):1873–8.
[12] Mao H, Driscoll SJ, Li JS, Li G, Wood KB, Cha TD. Dimensional changes of the neuroforamina in subaxial cervical spine during in vivo dynamic flexion-extension. Spine J 2016 Apr;16(4):540–6.
[13] Schell A, Rhee JM, Holbrook J, Lenehan E, Park KY. Assessing foraminal stenosis in the cervical spine: a comparison of three-dimensional computed tomographic surface reconstruction to two-dimensional modalities. Global Spine J 2017 May;7(3):266–71.
[14] Kuijper B, Beelen A, van der Kallen BF, Nollet F, Lycklama A, Nijeholt GJ, de Visser M, Tans JT. Interobserver agreement on MRI evaluation of patients with cervical radiculopathy. Clin Radiol 2011 Jan;66(1):25–9.
[15] Kobayashi R, Iizuka H, Nishinome M, Iizuka Y, Yorifuji H, Takagishi K. A cadaveric study of the cervical nerve roots and spinal segments. Eur Spine J 2015 Dec;24(12):2828–31.
[16] Tanaka N, Fujimoto Y, An HS, Ikuta Y, Yasuda M. The anatomic relation among the nerve roots, intervertebral foramina, and intervertebral discs of the cervical spine. Spine (Phila Pa 1976) 2000 Feb 1;25(3):286–91.
[17] Epstein JA, Lavine LS, Aronson HA, Epstein BS. Cervical spondylotic radiculopathy. The syndrome of foraminal constriction treated by foramenotomy and the removal of osteophytes. Clin Orthop Relat Res 1965 May-Jun;40:113–22.
[18] Kang MS, Choi KC, Lee CD, Shin YH, Hur SM, Lee SH. Effective cervical decompression by the posterior cervical foraminotomy without discectomy. J Spinal Disord Tech 2014 Jul;27(5):271–6.
[19] Gu BS, Park JH, Seong HY, Jung SK, Roh SW. Feasibility of posterior cervical foraminotomy in cervical foraminal stenosis: prediction of surgical outcomes by the foraminal shape on preoperative computed tomography. Spine (Phila Pa 1976) 2017 Mar;42(5):E267–71.

Please cite this article as: Mizouchi T et al., Three-dimensional morphological analysis of cervical foraminal stenosis using dynamic flexion-extension computed tomography images, Journal of Orthopaedic Science, https://doi.org/10.1016/j.jos.2019.11.002